Metabolic Engineering 11 (2009) 107–116

Contents lists available at ScienceDirect

Metabolic Engineering

journal homepage: www.elsevier.com/locate/ymben

Overexpression of isocitrate lyase—glyoxylate bypass influence on metabolism in *Aspergillus niger*

S. Meijer [1], J. Otero, R. Olivares, M.R. Andersen, L. Olsson [2], J. Nielsen *,[2]

Department for Systems Biology, Center for Microbial Biotechnology, Building 223, Technical University of Denmark, DK-2800 Kgs Lyngby, Denmark

ARTICLE INFO

Article history:
Received 27 June 2008
Received in revised form
17 November 2008
Accepted 16 December 2008
Available online 20 January 2009

Keywords:
Isocitrate lyase over-expression
Glyoxylate bypass
Reduced organic acids
Metabolic network analysis
Gene expression

ABSTRACT

In order to improve the production of succinate and malate by the filamentous fungus *Aspergillus niger* the activity of the glyoxylate bypass pathway was increased by over-expression of the isocitrate lyase (*icl*) gene. The hypothesis was that when isocitrate lyase was up-regulated the flux towards glyoxylate would increase, leading to excess formation of malate and succinate compared to the wild-type. However, metabolic network analysis showed that an increased *icl* expression did not result in an increased glyoxylate bypass flux. The analysis did show a global response with respect to gene expression, leading to an increased flux through the oxidative part of the TCA cycle. Instead of an increased production of succinate and malate, a major increase in fumarate production was observed.

The effect of malonate, a competitive inhibitor of succinate dehydrogenase (SDH), on the physiological behaviour of the cells was investigated. Inhibition of SDH was expected to lead to succinate production, but this was not observed. There was an increase in citrate and oxalate production in the wild-type strain. Furthermore, in the strain with over-expression of *icl* the organic acid production shifted from fumarate towards malate production when malonate was added to the cultivation medium.

Overall, the *icl* over-expression and malonate addition had a significant impact on metabolism and on organic acid production profiles. Although the expected succinate and malate formation was not observed, a distinct and interesting production of fumarate and malate was found.

1. Introduction

For decades microbial citric acid production has been an important industrial process. The main source for citric acid production is the filamentous fungus *Aspergillus niger*. Medium composition and technical parameters have been extensively characterised and adapted to create an optimal production process (Kristiansen et al., 1999; Papagianni, 2007). With advances in molecular biology and functional genomics during the last years it has become possible to study metabolism at a global level. One important breakthrough has been the sequencing of the *A. niger* genome (Baker, 2006; Pel et al., 2007) and the subsequent design of DNA microarrays (Andersen et al., 2008). Another important and powerful method is metabolic network analysis, which has proven to be an important tool for analysis of the metabolic network and cellular physiology (Christensen and Nielsen, 1999; Schmidt et al., 1997; Zupke and Stephanopoulos, 1994). For quantifying metabolic fluxes, measurements of the amino acid labelling patterns by GC–MS or NMR are required, using ^{13}C-labelled carbon sources. Quantification of the fluxes provides a direct measure of the degree of engagement of various pathways on the overall cellular function.

Using DNA microarrays and flux analysis it is possible to get an in-depth knowledge about which molecular and biochemical pathways play a key role in product formation. Especially, in the quest to develop generic cell factories used for the production of a wide range of products, it is necessary to obtain detailed knowledge of the working mechanism of metabolic networks. The main focus of the present study is on the central carbon metabolism and the organic acid production in *A. niger*. With the ability of this fungus to produce high amounts of citric acid, it represents an attractive cell factory for the production of other organic acids like malic, fumaric and succinic acid. They are all considered valuable for the chemical industry (Werpy and Petersen, 2004). For the production of these four-carbon organic acids it is quite natural to study the role of the glyoxylate pathway, as this pathway leads to malic acid and succinic acid production (Bowyer et al., 1994). Therefore, it was attempted to redirect fluxes towards the glyoxylate pathway by over-expressing the isocitrate lyase (ICL). ICL is the first enzyme of the glyoxylate pathway, with

* Corresponding author. Fax: +46 31 772 38 01.
E-mail address: nielsenj@chalmers.se (J. Nielsen).
[1] Current address: Sandoz GmbH, Kundl, Austria.
[2] Current address: Department of Chemical and Biological Engineering, Chalmers University of Technology, Kemivägen 10, 412 96 Gothenburg, Sweden.

1096-7176/$ - see front matter © 2009 Elsevier Inc. All rights reserved.
doi:10.1016/j.ymben.2008.12.002

malate synthase being the second enzyme. The effect of adding malonic acid to the medium was also investigated. Malonic acid is known to be an inhibitor of succinate dehydrogenase (SDH). By disrupting the TCA cycle we tried to produce more organic acids in the form of succinic acid and malic acid.

The influence of *icl* over-expression and malonic acid addition on cellular performance was determined by transcript levels using DNA microarrays and metabolic flux analysis. Additionally, activities of key enzymes in the pathways leading to organic acids, as well as extracellular metabolite levels were measured. Our goal was to link the different information levels (genome, transcriptome, enzyme activities, metabolome and fluxome) to obtain a system-level understanding of the effect of *icl* over-expression on the cellular physiology. This provided us with new insights into the regulation of metabolism that can be used for improving the organic acid production of succinate and malate in the filamentous fungus *A. niger*.

2. Materials and methods

2.1. Strains

As reference strain the laboratory strain N402 of *A. niger* was used. The *icl* over-expression was made in the *pyrA*-strain AB4.1, which is auxotrophic for uridine and uracil. The *icl* gene was put on a high copy number plasmid. The vector used was pCR2.1-AfpyrG (kindly provided by Axel Brakhage), which carries *pyrG* from *A. fumigatus* (Vanhartingsveldt et al., 1987). *Icl* was fused to the *A. nidulans gpdA* promoter using fusion PCR. PCR was performed using the Expand High Fidelity PCR kit (Roche) according to the manufacturer's recommendations. The primers used are shown in Table 1. The fusion PCR product of *gpdA* and *icl* was cut with SbfI, and the pCR2.1-AfpyrG vector was cut with PsiI. Both these enzymes are blunt-end cutting restriction enzymes and therefore the pCR2.1-AfpyrG vector and *icl* fusion gene product can be ligated using T4 DNA ligase. The ICL over-expression plasmid pCR2.1-AfpyrG_ICL was transformed into the AB4.1 strain using the protoplast and transformation procedures for *A. niger* as described previously for *A. nidulans* (Nielsen et al., 2006).

2.2. Cultivation media

For the pre-culture a defined medium was used containing 10 g/L D-glucose, 50 ml salt solution, 1 ml trace element solution 1 and 18 g/L agar. The salt solution contained 120 g/L $NaNO_3$, 10.4 g/L KCl, 10.4 g/L $MgSO_4 \cdot 7H_2O$ and 30.4 g/L KH_2PO_4. The trace element solution 1 contained 22 g/L $ZnSO_4 \cdot 7H_2O$, 11 g/L H_3BO_3, 5 g/L $MnCl_2 \cdot 2H_2O$, 5 g/L $FeSO_4 \cdot 7H_2O$, 1.7 g/L $CoCl_2 \cdot 6H_2O$, 1.6 g/L $CuSO_4 \cdot 5H_2O$, 1.5 g/L $Na_2MoO_4 \cdot 2H_2O$ and 50 g/L Na_4EDTA. Spores were propagated on agar plates containing this medium at pH 6.5.

Table 1
Primers used for fusion PCR to over-express *icl* in *A. niger*.

Primer name	Sequence
GpdA_up	AATAT **CCTGCAGG** GCT GAT TCT GGA GTG ACC CAG AG
GpdA_down	CTT CTT CTT CAA AGG AAG CCA T ACA CCG GGC GGA CAG ACG
ICL_up	ATG GCT TCC TTT GAA GAA GAA G
ICL_down	ATTA **CCTGCAGG** ATT CCC CTC CAT TCC CAT GC

The underlined letters are the overlapping genetic elements used for fusion PCR. The bold letters code for the restriction enzyme Sbf1 that is used for restriction of the fusion PCR product, before insertion in the pCR2.1-AfpyrG plasmid.

The batch cultivations were carried out in a chemically defined medium adjusted to pH 2.5 containing 10 g/L glucose, 10 g/L $NaNO_3$, 3 g/L KH_2PO_4, 2 g/L $MgSO_4 \cdot 7H_2O$, 2 g/L NaCl, 0.2 g/L $CaCl_2 \cdot 2H_2O$, 0.5 ml/L antifoam (sb2121) and 1 ml/L trace element solution 2. The trace element solution 2 contained 14.3 g/L $ZnSO_4 \cdot 7H_2O$, 2.5 g/L $CuSO_4 \cdot 5H_2O$, 0.5 g/L $NiCl_2 \cdot 6H_2O$, 7 g/L $MnCl_2 \cdot 2H_2O$ and 13.8 g/L $FeSO_4 \cdot 7H_2O$.

These cultivations were used for microarray analysis, enzyme analysis and metabolite analysis and were run in triplicate for each of the 4 conditions.

For the flux experiments 5 g/L of 1-^{13}C glucose was used as sole carbon source. The rest of the medium components were the same as described above. The same reactor was used in all other experiments, only the working volume was reduced to 200 mL for the flux experiment. The flux experiment was performed once with sampling at multiple time points where at least 3 time points were taken in the pseudo-steady-state condition.

2.3. Cultivation conditions

Before spore harvesting with 0.01% Tween-80 the pre-culture plates were incubated for 4–7 days at 30 °C. Subsequently, 10^9 spores were inoculated in 3 L Braun bioreactors with a working volume of 2 L. The temperature was maintained constant at 30 °C and the pH was controlled by automatic addition of 1 M $NaCO_3$ or 2 M HCl. Two Rushton four-blade disc turbines were used for homogeneous mixing. No baffles were used in the reactors thereby reducing the surface area available for biofilm formation. The initial aeration rate, agitation and pH were 0.2 vvm, 200 rpm and pH 2.5, respectively. They were gradually changed after germination (that takes place after approximately 15 h) to 0.02 vvm, 700 rpm and pH 5, respectively. These parameters were kept constant throughout the rest of the batch cultivation. Air was used for sparging and the concentrations of oxygen and carbon dioxide in the exhaust gas were monitored by an acoustic gas analyser (Brüel & Kjær, Nærum, Denmark). The dissolved oxygen tension (DOT) was measured with an oxygen probe (Mettler Toledo sensors).

2.4. Sampling

Biomass samples were taken manually from the reactor. For dry weight measurements, a known cell culture volume was filtered through a pre-weighed nitrocellulose filter (pore size 45 μm, Pall Corporation). The filtrate was frozen immediately and later used for the determination of the concentrations of substrate and extracellular metabolites. The filter was washed with 0.9% w/v NaCl, dried for 15 min in a microwave oven at 150 W and weighed again to determine the biomass concentration.

For determination of *in vitro* enzyme activities, biomass samples were filtered through a nitrocellulose filter (pore size 45 μm, Pall Corporation) and washed with 0.9% w/v NaCl. The filter cake ($\pm$1 g) was immediately frozen in liquid nitrogen and stored at −80 °C. For flux analysis the biomass samples were quickly filtered and immediately quenched in liquid nitrogen. The samples taken for microarray determination were immediately quenched in liquid nitrogen without any filtration of the biomass samples.

2.5. Substrate and extracellular metabolite quantification

High-performance liquid chromatography was used for the quantification of extracellular sugars and organic acids. Glucose, acetate, pyruvate, citrate, ethanol, succinate, fumarate, malate, glycerol and oxalate concentrations were measured on an Aminex

HPX-87H cationic exchange column (BioRad, Hercules, CA, USA) eluted at 60 °C with 5 mM H_2SO_4 at a flow rate of 0.6 mL/min. Metabolites were detected with both a refractive index detector and a UV detector.

2.6. Analysis of in vitro enzyme activities

The frozen samples were crushed on liquid nitrogen with a mortar. The crushed biomass (0.5 g) was dissolved in 2 mL of extraction buffer containing 25 mM MES-NaOH, 0.1 mM EDTA, 0.1 mM DTT, 0.1 mM phenylmethylsulfonyl fluoride and 0.1 mM NaN_3. This solution was transferred to 2 mL FastPrep tubes containing 0.5 mL glass beads (0.75–1 mm). The FastPrep tubes were processed 3 times 10 s on a FastPrep FP120 Instrument (Savant Instruments, New York, USA), at speed setting 5, with cooling on ice in between. After disruption, samples were centrifuged at 13,000*g* at 4 °C for 10–20 min, and the supernatants were analysed for enzyme activity.

Enzyme assays were performed at 30 °C using a HP8453 UV–visible light spectrophotometer. In order to test the linearity of the assays, the reactions were performed with 2–3 different dilutions of cell extract. The specific enzyme activities were expressed in micromoles $min^{-1} mg^{-1}$ (U/mg). The amount of protein was determined by the Bradford method with bovine serum albumin as the standard (Bradford, 1976). Four different enzyme activities were measured: citrate synthase (CIT), malate dehydrogenase (MDH), isocitrate lyase and pyruvate carboxylase (PYC) as described by Meijer et al. (2007).

2.7. Determination of intracellular flux distribution

2.7.1. Sample preparation and derivatisation for flux analysis

The 35–50 mg of biomass was dissolved in 600 µl 6 M HCl and kept overnight at 105 °C for hydrolysis. The hydrolysate was then centrifuged for 5 min at 15,000 rpm and the supernatant was transferred into new vials. The supernatant was dried for 3 h at 105 °C and dissolved in 200 µl milliQ water.

In the mean time, the resin bed for solid phase extraction was prepared by weighing 1 g of Dowex cation exchange resin and mixed with 15 mL of 50% w/w glycerol. The 1 mL of resin solution was added to a syringe containing a frit on a SPE workstation. When the resin was settled at the bottom of the syringe, the excess of glycerol was drained and a second frit was added on top of the resin. The 2 mL of biomass hydrolysate was added on the SPE column. After the biomass had trickled through the column, 1 mL of 50% v/v ethanol solution was added followed by 200 µL 1 M NaOH solution, which washed the remaining unbound compounds off the column. Finally, the amino acids were eluted with 1 mL of solution containing 1% v/v NaOH in saline (0.9% w/v NaCl), ethanol and pyridine in a ratio of 9:5:1, respectively. The eluted amino acids were derivatised by two separate methods.

(1) ethylchloroformate (ECF) derivatisation and
(2) dimethylformamide dimethylacetal (DMF/DMA) derivatisation.

In the ECF derivatisation 50 µL ECF was added to 500 µL amino acid solution and mixed in two sequential rounds of 30 s. Next, 200 µL propylacetate was added and finally 50 µL 1 M HCl. The upper organic layer was removed and analysed by GC–MS.

The DMF/DMA derivatisation required the addition of 300 µL 1 M HCl to 500 µL amino acid solution followed by a 2–4 h drying period at 105 °C. 200 µL DMF/DMA and 200 µL acetonitrile were then added to dissolve the dried substance and mixed well for 30 s. This solution was kept at 100 °C for 20 min and was subsequently transferred to −20 °C for 10 min to ensure proper derivatisation. This solution was finally analysed by the GC–MS.

2.7.2. GC–MS analysis

GC–MS analysis was performed on an Agilent (Palo Alto, CA, USA) HP 6890 gas chromatograph coupled to a HP 5973 quadrupole mass selective detector in positive electron impact ionization (EI^+) operated at an electron energy of 70 eV. The GC was equipped with a 4.0 mm i.d. Siltek gooseneck splitless deactivated liner (Restek, Bellefonte, PA, USA), and a Supelco (Bellefonte, PA, USA) SLB-5 MS column, 15 m, 0.25 mm i.d., 0.25 µm film. Helium of a purity of 99.999% was used as carrier gas at a constant linear gas velocity of 35 cm/s. Transfer line temperature was 280 °C, quadrupole temperature 150 °C and MS source 200 °C. The GC–MS system was controlled from Agilent MSD Chemstation v. D.01.02.16. For both methods (ECF and DMF/DMA) 1 µL sample was injected in the splitless (30 s, split 1:20) mode at 200 °C using a hot needle. The MS scan range was m/z 40–400 with 2.88 s/scan. To avoid sample carry-over the syringe was cleaned using five times 5 µL acetone, then five times 5 µL dichloromethane and finally 3 times rinsing with 3 µL sample.

2.7.3. ECF derivatives

The oven temperature was initially held at 75 °C for 1 min. Hereafter, the temperature was raised with a gradient of 40 °C/min until 165 °C, after which the temperature increase was 4 °C/min until 190 °C and followed by an increase of 40 °C/min up to 240 °C. Finally, the temperature was increased to 260 °C with a gradient of 4 °C/min and held constant for 4 min. The flow through the column was held constant at 1.3 mL He/min. The temperature of the inlet was 200 °C, of the interface 280 °C and of the quadrupole 105 °C.

2.7.4. DMF/DMA derivatives

Initially, the oven temperature was held at 60 °C for 1 min. Hereafter, the temperature was raised with a gradient of 20 °C/min until 130 °C, after which the temperature increase was 4 °C/min until 150 °C and followed by an increase of 40 °C/min up to 260 °C. Next, this temperature was held constant for 4.25 min. The flow through the column was held constant at 1 mL He/min. The temperature of the inlet was 230 °C, of the interface 270 °C and of the quadrupole 105 °C.

2.7.5. Metabolic network analysis

The flux analysis was based on the labelling patterns of derivatives of glucose and amino acids obtained from acid hydrolysis of the biomass. The mass spectra obtained from the GC–MS were converted into summed fractional labelling (SFL) patterns with the aid of the XCMS library operating within the R programming language environment (Smith et al., 2006). The SFL of a molecule or a fragment is identical to the sum of the fractional labelling of the carbon atoms contained in the molecule or fragment.

The metabolic network consisted of 52 reactions, 6 of them are reversible and 25 balanced metabolites (see Supplementary material S2). The fluxes were determined using an in-house program code in Matlab V 7.0.4 (Grotkjaer et al., 2005), which implements the metabolic network analysis framework from Wiechert (2001). The algorithm minimises the differences between measured fluxes and calculated fluxes by least-square minimisation, as well as measured and calculated SFL using the non-linear Levenberg–Marqueartd algorithm. Measured fluxes were weighed with a standard deviation of 10%. Multiple initial guesses were generated with a genetic algorithm to verify the existence of a global minimum. A sensitivity analysis was done by

adding 10% of Gaussian noise to the measured SFL data in 50 simulations followed by calculating the standard deviation of the estimated fluxes.

2.8. Analysis of transcription data

2.8.1. Total RNA extraction

Total RNA was extracted from 40 to 50 mg frozen mycelia. The mycelia were transferred to pre-cooled 2 ml Eppendorf tubes containing steel balls (2 × ∅2 mm, 1 × ∅5 mm) and shaken in a Mixer Mill for 10 min at 4 °C. The resulting powder was used for total RNA extraction using the Qiagen RNA easy kit, according to the protocol for isolation of total RNA from plant and fungi.

The quality of the extracted total RNA of each sample was analysed using the Bioanalyser 2100 (Agilent technologies Inc., Santa Clara, CA, USA) and the quantity of the extracted total RNA was determined spectrophotometrically (Amersham Pharmacia Biotech, GE Healthcare Biosciences AB, Uppsala, Sweden). The total RNA was stored at −80 °C until further processing.

2.8.2. Biotin labelled cRNA and microarray processing

The 5 μg of total RNA was used for making 15 μg of fragmented biotin labelled cRNA that was hybridised to the 3AspergDTU gene chip (Affymetrix) according to the Affymetrix GeneChip Expression Analysis Technical Manual (Affymetrix, 2007). The cRNA quality and quantity were analysed in the same way as the total RNA described above. A GeneChip fluidics Station FS-400 and a GeneChip scanner were used for hybridisation and scanning of the microarrays. The scanned probe array images were converted to .CEL files using the GeneChip Operating Software (Affymetrix). Affymetrix CEL-data files were pre-processed using the statistical language and environment R (R Development Core Team, 2007). The probe intensities were normalised for background using the robust multiarray average (RMA) method (Irizarry et al., 2003) only using perfect match (PM) probes. Subsequently, normalisation was performed using the quantiles algorithm (Bolstad et al., 2003). Gene expression values were calculated from the PM probes with the medianpolish summary method (Irizarry et al., 2003). All statistical pre-processing methods were used by invoking them through the Affymetrix package (Gautier et al., 2004).

Statistical analysis was applied to determine genes subject to differential transcriptional regulation. The limma package (Smyth, 2004) was used for all statistical analyses. Moderated *t*-tests between the sets of experiments were used for pair-wise comparisons. Empirical Bayesian statistics were used to moderate the standard errors within each gene and Benjamini–Hochberg's method (Benjamini and Hochberg, 1995) was used to adjust for multi-testing. A cut-off value of adjusted $p<0.05$ was used for statistical significance. The significantly expressed genes can be found in Supplementary material S1.

3. Results and discussion

Because most living cells are capable of using a large variety of compounds as carbon, energy and nitrogen sources, they contain complementary pathways that serve similar functions when they operate at the same time. The glyoxylate bypass can be seen as a bypass pathway of the TCA cycle, because the two pathways share a number of similar reactions. In prokaryotes these two pathways are both present in the cytosol, while in eukaryotes compartmentalisation separates them. The TCA cycle is located in the mitochondria, in contrast to the glyoxylate bypass that operates either in the cytosol or in microbodies. Although these pathways follow the same reactions they serve very different purposes. The TCA cycle serves as an oxidising pathway where pyruvate is converted to carbon dioxide, whereas the glyoxylate bypass has the purpose of synthesising precursor metabolites anaplerotically, e.g. net production of oxaloacetate from acetyl-CoA. The glyoxylate bypass basically consists of only two enzymes: isocitrate lyase (EC 4.1.3.1) and malate synthase (MS, EC 2.3.3.9) (Kornberg and Krebs, 1957). ICL catalyses the cleavage of isocitrate to succinate and glyoxylate and hence, isocitrate is a branch point metabolite between the TCA cycle and the glyoxylate bypass. MS catalyses the condensation of acetyl-CoA and glyoxylate to form malate. This anaplerotic reaction enables a net synthesis of C_4 carboxylic acids from a carbon source of C_2 compounds like acetate or fatty acid derived acetyl-CoA (Kornberg, 1966). In the present study the *icl* gene was over-expressed in order to stimulate the glyoxylate bypass flux and thereby produce more succinate and malate in *A. niger*.

Unfortunately a comparison between an ICL deletion strain, the wild type strain and an ICL over-expression strain could not be performed in this study since the gene targeting in *A. niger* is quite difficult, and we could therefore not construct a deletion strain.

3.1. Comparison of WT and ICL over-expression strains

The wild-type strain and the ICL over-expression mutant were grown in batch cultures with glucose as carbon source. Metabolic fluxes were determined, as well as the global transcription response using DNA microarrays. Based on the data, 1511 significantly changed genes were identified using a moderated *t*-test. The list of significantly changed genes is given in Supplementary material S1.

The metabolic flux analysis showed that in the ICL over-expression strain the flux towards the PPP is reduced (Fig. 1). The total flux through the glycolysis was increased. At the branch point towards serine synthesis a higher flux towards serine was measured in the ICL over-expression strain compared to the WT strain. Fig. 1 is a simplified representation of the stoichiometric metabolic model. The complete model can be found in Supplementary material S2. The microarray data support the decreased flux in the PPP since the genes in the PPP were significantly down-regulated. Furthermore, genes encoding glycolytic enzymes were up-regulated whereas gluconeogenic genes were down-regulated, supporting the increased glycolytic flux (Fig. 1). Glycolysis is known to be important for citrate production since most of the citrate is produced through this pathway (Cleland and Johnson, 1954; Martin and Wilson, 1951; Legisa and Mattey, 1986). Only a slight increase in citrate yield was found in the ICL over-expression strain (0.05 C-mol/C-mol glucose in the WT and 0.14 C-mol/C-mol glucose in the ICL over-expression strain), indicating that the over-expression changed the flux distribution (Table 2). Looking at the fermentation profiles a higher citrate concentration was measured during the exponential growth phase (Fig. 2).

For the TCA cycle a similar positive correlation between transcription and flux was not found. The flux through the TCA cycle was lower in the ICL over-expression strain compared to the wild-type strain, while expression of several of the TCA cycle genes was up-regulated. Over-expression of the *icl* was not confirmed by the gene expression data. The expression levels of *icl* and *ms* were only slightly increased (fold change is 1.1). This is likely to be an artefact as a higher ICL enzyme activity was observed in the over-expression strain (Table 3). In order to confirm ICL over-expression a semi-quantitative reverse transcriptase PCR reaction was performed using the SuperScript III

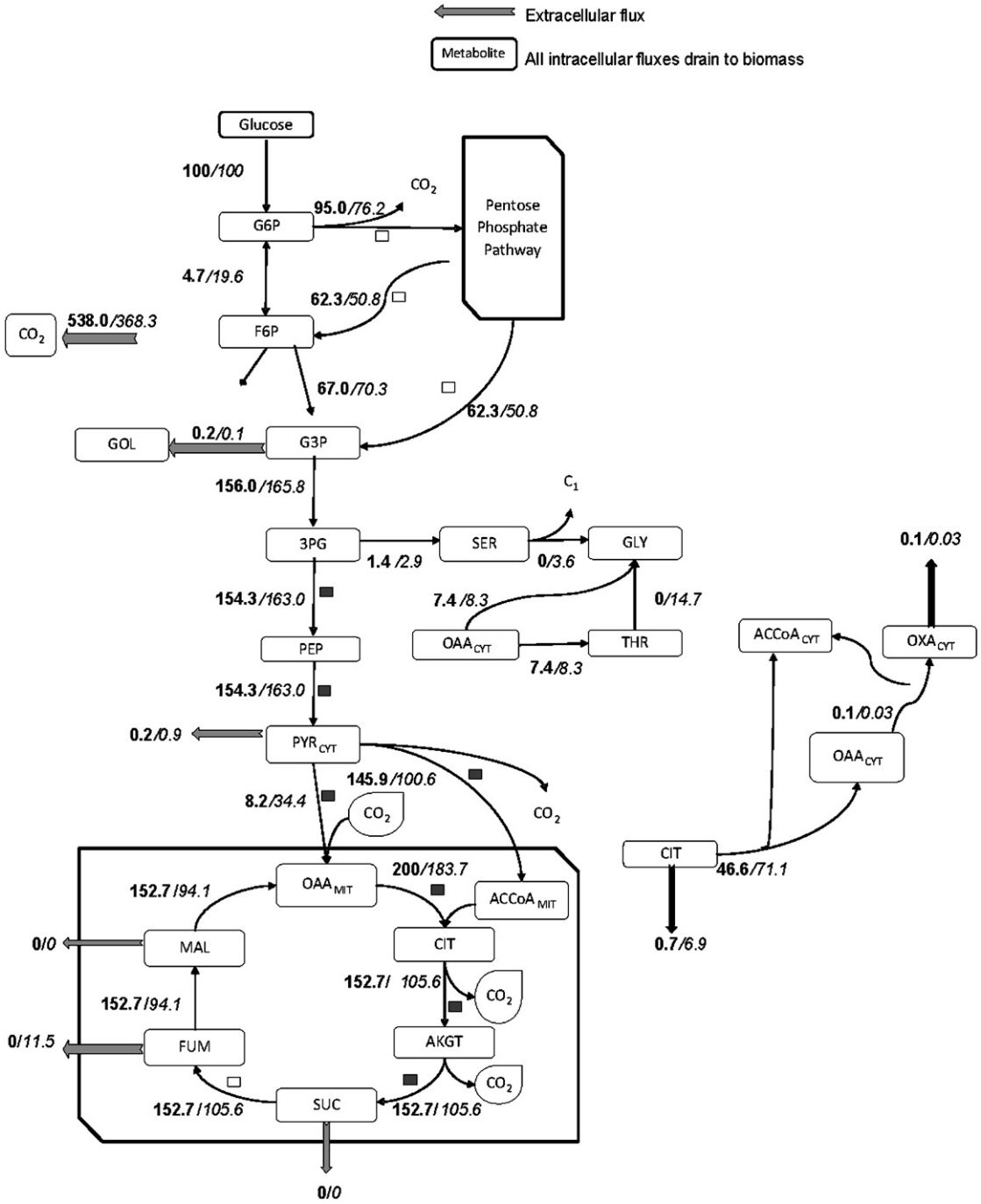

Fig. 1. A simplified flux distribution model of the WT (N402) and ICL over-expression strain (complete model see S2). The first number is the flux in the N402 strain and the second number (italic) is the flux in the ICL over-expression strain. G6P = glucose-6-phosphate, F6P = fructose-6-phosphate, GOL = glycerol, G3P = glyceraldehydes-3-phosphate, PEP = phosphoenolpyruvate, PYRcyt = cytosolic pyruvate, SER = serine, GLY = glycine, THR = threonine, OAAcyt = cytosolic oxaloacetate, CIT = citrate, ACCoAcyt = cytosolic acetyl-CoA, OXAcyt = cytosolic oxalate, ACCoAmit = mitochondrial acetyl-CoA, OAAcyt = mitochondrial oxaloacetate, AkGT = alfa-keto-glutarate, SUC = succinate, FUM = fumarate, MAL = malate. Up-regulation of gene expression levels (■) and down-regulation of gene expression levels (□). Unmarked reactions did not have any significant change in gene expression.

OneStep RT-PCR kit (Invitrogen) following the manufacturer's protocol. This experiment showed that ICL was up-regulated (data not shown).

The fumarate reductase was found to be down-regulated, but nevertheless no succinate production was observed in the ICL over-expression strain (Table 2). Succinate production could result from up-regulation of the oxidative part of the TCA cycle and down-regulation of the gene encoding fumarate reductase. However, instead of producing succinate and malate, the estimated fluxes and measurements of the extracellular metabolite concentrations indicated that fumarate was over-produced. This suggests that instead of up-regulating the glyoxylate bypass by over-expressing the *icl* gene, the oxidative part of the TCA cycle is up-regulated, creating a bottleneck in the TCA cycle, leading to fumarate production. In comparison to the WT, the ICL over-expression strain produced more fumarate and pyruvate, and less oxalate and glycerol (Fig. 1 and Table 2) indicating a clear shift of flux distribution in the TCA cycle.

Table 2
Biomass and organic acid yields expressed in C-mol/C-mol glucose consumed.

	Biomass	Citric acid	Oxalic acid	Succinic acid	Pyruvic acid	Glycerol	Fumaric acid
WT	0.37±0.07	0.05±0.009	0.016±0.005	0.003±0.001	0.0012±0.006	0.0032±0.0008	0
WT+mal	0.23±0.06	0.08±0.01	0.030±0.004	0	0	0.0032±0.0005	0
ICL	0.22±0.09	0.14±0.04	0	0	0.033±0.011	0	0.058±0.02
ICL+mal	0.58±0.11	0.09±0.007	0	0	0.0025±0.007	0.0059±0.0007	0.003±0.002

WT = wild-type N402 strain, WT+mal = N402 strain with addition of 50 mM malonate, ICL = isocitrate lyase over-expression in the AB4.1 strain, ICL+mal = isocitrate lyase over-expression in the AB4.1 strain with addition of 50 mM malonate.

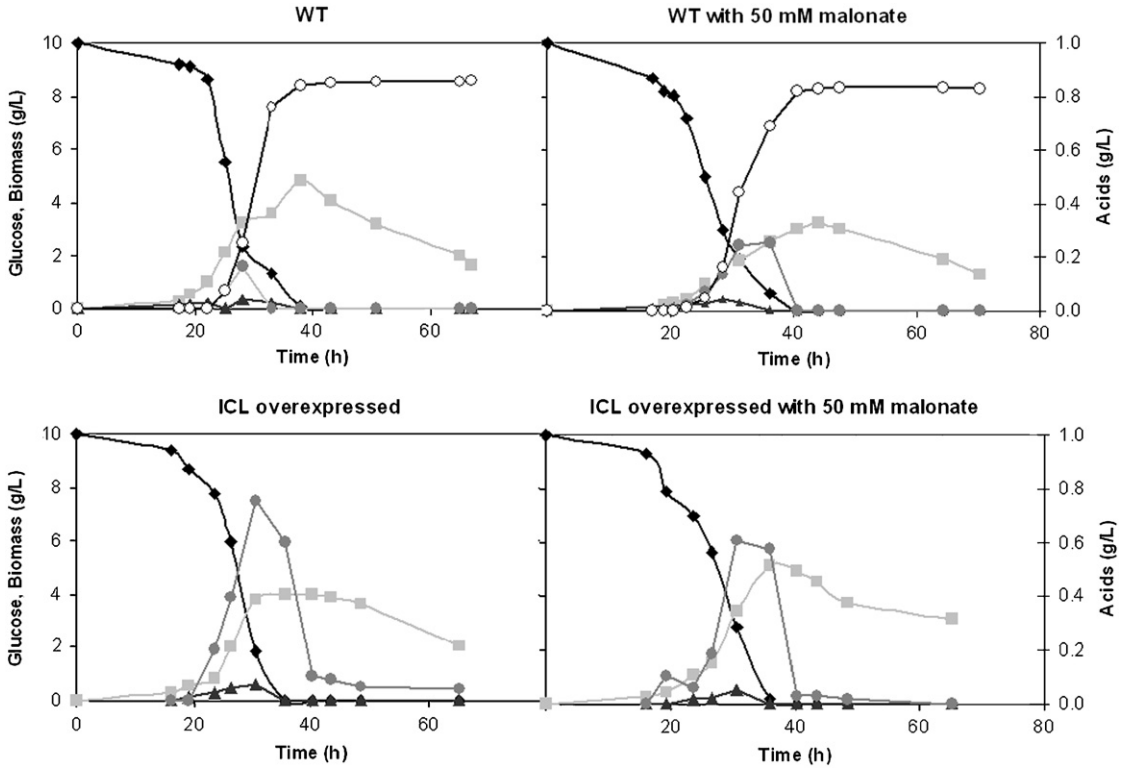

Fig. 2. Fermentation profiles of the wild-type N402 strain and ICL over-expression strain with and without 50 mM malonate addition in glucose batches. ◆ = Glucose, ■ = biomass, ● = citrate, ▲ = glycerol and ○ = oxalate.

Table 3
Enzyme activities in U/mg measured in different *A. niger* strains.

	ICL	MDH	CIT	PYC
WT	0.26	0.016	0.10	0.013
WT+mal	0.1	0.012	0.07	0.031
ICL	0.38	0.009	0.14	0.023
ICL+mal	0.47	0.003	0.06	0.029

WT = wild-type N402 strain, WT+mal = N402 strain with addition of 50 mM malonate, ICL = isocitrate lyase over-expression in the AB4.1 strain, ICL+mal = isocitrate lyase over-expression in the AB4.1 strain with addition of 50 mM malonate.
ICL = isocitrate lyase, MDH = malate dehydrogenase, CIT = citrate synthase, PYC = pyruvate carboxylase.

The *in vitro* enzyme activities measured in the ICL over-expression strain differed from the WT (Table 3). First, measurement of the ICL activity confirmed that the gene was over-expressed in the ICL strain as the activity was higher. Although the MDH activity was reduced, no malate or succinate was produced. The PYC activity was increased in the ICL over-expression strain, which corresponds with the increased gene expression and elevated flux through this pathway. The expression of the gene encoding pyruvate dehydrogenase (PDH) was also up-regulated, but this reaction showed a decreased flux in the ICL over-expression strain. Comparing the pyruvate carboxylase and pyruvate dehydrogenase flux at the pyruvate branch point in the ICL over-expression strain showed that the pyruvate dehydrogenase flux was higher than the carboxylase flux. Compared to the WT strain the ratio between dehydrogenase and carboxylase flux was found to be changed, but the dehydrogenase flux was still most dominant. This suggests that the oxidative TCA cycle is active, as this pathway requires both oxaloacetate and acetyl-CoA. The reduced flux through the TCA cycle in the ICL over-expression strain may be caused by a feedback regulation mechanism exerted at the level of the fumarase reaction that converts fumarate to malate.

A slightly higher citrate production in the ICL over-expression strain is likely to be caused by an increased formation of oxaloacetate. The rate of the reaction catalysed by citrate synthase is controlled *in vivo* by the oxaloacetate concentration. Oxaloacetate first binds to the enzyme, followed by binding of acetyl-CoA (Kubicek and Rohr, 1980; Papagianni, 2007). Therefore, if more

oxaloacetate is produced the production of citrate will also increase.

The measured gene expression data between the WT and ICL over-expression strain showed also pathway regulations outside the central carbon metabolism. The gene expression changes were mapped against the stoichiometric model developed by Andersen et al. (2008). These analyses showed that the protein degradation pathway was significantly down-regulated, whereas the purine and pyrimidine pathways were up-regulated in the ICL over-expression strain.

Since major changes were detected in the PPP and TCA cycle, which are pathways that are highly linked to redox reactions, it seems that the redox balance has been changed in the ICL over-expression strain. Führer et al. (1980) showed that a remarkable constancy was found in the catabolic reduction charge (NADH/(NADH+NAD)) and the anabolic reduction charge (NADPH/(NADPH+NADP)) in *A. niger* grown at non-limited growth conditions. Furthermore, they observed that the ratio (NAD+NADH)/(NADP+NADPH) was constant over the whole culture time. In the growth phase of *A. niger*, the catabolic reduction charge has been found to be relatively high (0.10) and during citric acid accumulation this value was even higher. This may reflect the metabolic situation of growth-restricting conditions necessary for acidogenesis (Kubicek and Rohr, 1977). Excessive NADH production under acidogenic conditions also requires high alternative oxidase activity (AOX) to maintain the redox balance and to limit the amount of ATP produced (Ruijter et al., 2002). Since a shift in organic acid production was detected in the ICL over-expression strain, a shift in the catabolic reduction charge is expected. This shift may result in an up-regulation of the purine and pyrimidine pathways. It has been proven that the levels of pyridine nucleotides are highly interdependent and their well-balanced ratios are necessary for optimal operation of the metabolic pathways (Führer et al., 1980), indicating that in the ICL over-expression strain a new physiological state was achieved. It was also observed that the expression levels of genes involved in nitrogen metabolism were up-regulated, which can be linked to the need of nitrogen incorporation in the pyridine nucleotides. Also gene expression levels of other pathways requiring nitrogen were up-regulated like pathways leading to several amino acids and vitamins, e.g. the biotin pathway. These pathways mainly lead to biomass formation, however, in our experiments the biomass yield was not increased in the ICL over-expression strain. This indicates that up-regulation does not result in increased fluxes through these pathways.

3.2. Effect of malonate addition for SDH inhibition

Malonate is known to be a competitive inhibitor of the succinate dehydrogenase. In rat and mammalian cells its inhibitory characteristics have been demonstrated (K_i values of 0.68 and 0.018 mM, respectively) (Armson et al., 1995; Hatefi and Stiggall, 1976). Since the enzyme assay for SDH was not sufficiently sensitive for analysis in the cell extracts of *A. niger* (most likely due to instability of the co-factor FAD) the inhibition constant of malonate on SDH could not be determined. Instead several concentrations of malonate were tested and the effect of malonate on growth was assessed (data not shown). The fact that *A. niger* is unable to grow anaerobically suggests that SDH is an essential enzyme required for cellular propagation. It was expected that inhibiting the SDH with malonate would inhibit the growth of *A. niger*. Indeed, it was observed that with increasing malonate concentrations the growth was limited. A malonate concentration of 50 mM was found to be suitable for partial inhibition of SDH without having a considerable effect on the growth of *A. niger*. This concentration is much higher than the K_i values in rat and mammals, suggesting that there is some inhibition of the SDH enzyme. In order to be sure that malonate was reaching the SDH inside the cell, the uptake of malonate was verified by measurement of the intracellular levels of malonate. Hereby the effect of inhibition of SDH in the WT and the ICL over-expression strain could be evaluated. The effect between the strains was found to differ significantly.

Malonate addition affected the fluxes in the PPP and the fluxes towards amino acids (Figs. 3 and 4). When malonate was added in the WT strain the flux through the PPP was reduced and the flux towards amino acids was unchanged. In the ICL over-expression strain malonate addition caused an increase in the PPP flux. It was remarkable that in the ICL over-expression strain the flux towards amino acids was already higher compared to the WT strain. This flux increased even more when malonate was added. This increase in amino acid synthesis and PPP flux was accompanied by a significantly higher biomass yield of 0.58 C-mol biomass/C-mol glucose in the ICL over-expression strain when malonate was added, compared to 0.22 if no malonate was added (Table 2).

When malonate was added, the flux towards glycerol was increased while the extracellular pyruvate flux was decreased in both the WT and the ICL over-expression strain. This indicates that malonate addition regulates cell metabolism not only in the TCA cycle, but also in glycolysis.

At the pyruvate node, the flux ratio between pyruvate carboxylase and pyruvate dehydrogenase was changed. When malonate was added the flux through pyruvate carboxylase increased, and the flux ratio of PDH over PYC changed from 18 to 0.8 in the WT strain and from 3 to 0.2 in the ICL over-expression strain. This may indicate an increase in flux towards the reductive TCA cycle.

In the WT strain, the flux through the TCA was not significantly changed by adding malonate and the extracellular organic acid profiles were also not significantly changed, except for citrate and oxalate (Fig. 3 and Table 2). The increase in citrate flux upon addition of malonate did not relate to the 1.5-fold decrease in enzyme activity (Fig. 3 and Table 3).

In the ICL over-expression strain, the malonate addition did not lead to an increased flux towards citrate, rather a decreased flux (Fig. 4). When *icl* was over-expressed an almost 20 times increase in fumarate yield was detected (Table 2). This might be caused by a limitation in the conversion from fumarate to malate. When malonate was added, the flux control was shifted due to inhibition of the SDH activity. Therefore, instead of fumarate more malate was produced. The malate was most likely produced in the cytosol before it was shuttled towards the extracellular medium or towards the mitochondria in exchange for citrate. Since the citrate production was reduced the capacity of shuttling malate towards the mitochondria was decreased leading to more malate excretion into the medium.

The difference between the effect of malonate on the WT strain and ICL over-expression strain may be caused by a shift in flux control found in the metabolism. A strong flux control at the level of fumarase in the TCA cycle, caused by *icl* over-expression, was not present in the WT strain. The effect of SDH inhibition by malonate in the WT strain was therefore not effecting the fumarate and malate production, but instead increased the citrate and oxalate production.

4. Conclusion

Over-expression of the *icl* gene was hypothesised to up-regulate the glyoxylate bypass resulting in production of more succinate and malate. The glyoxylate bypass is known to be a

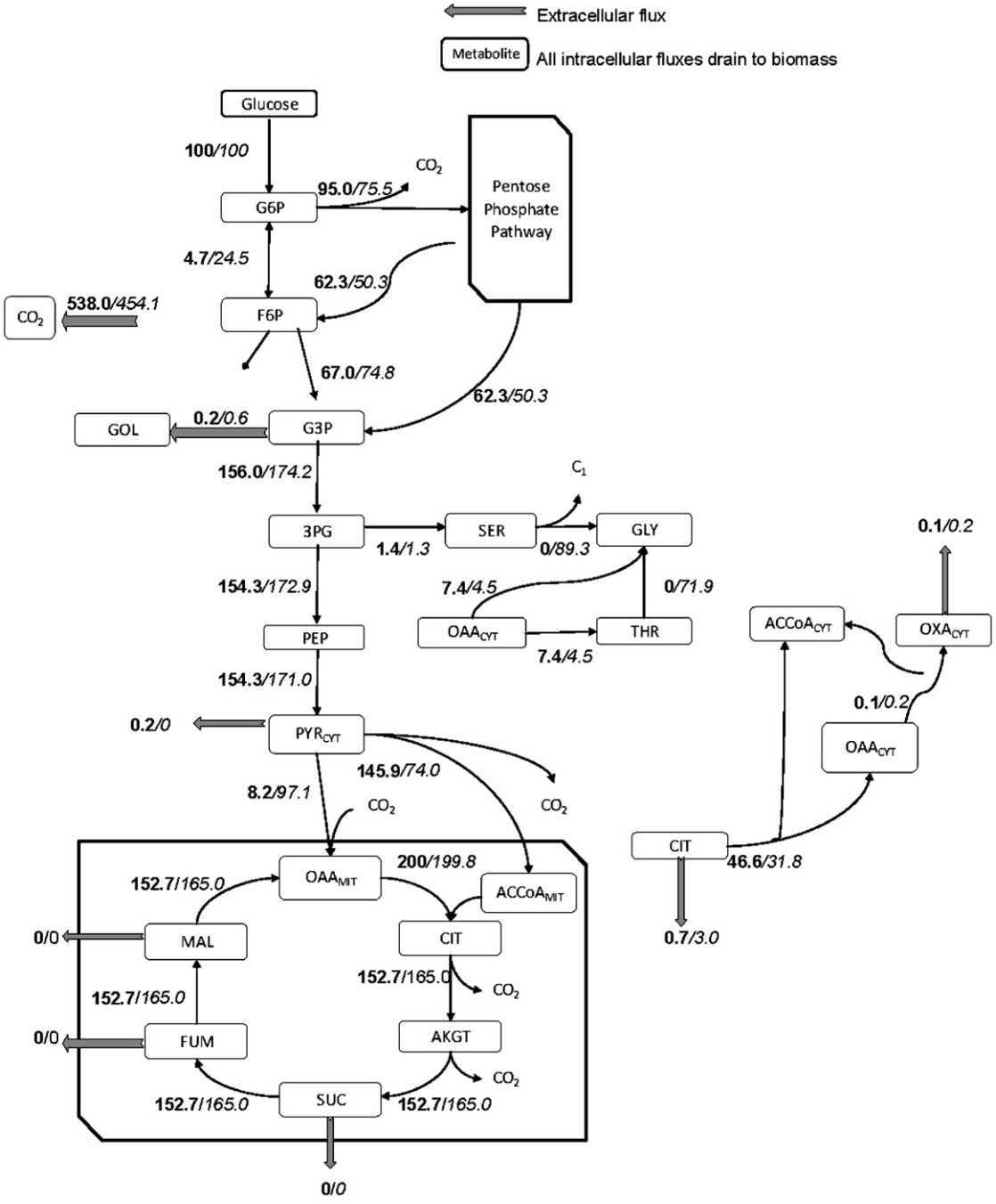

Fig. 3. A simplified flux distribution model of the wild-type N402 strain with and without 50 mM malonate addition (complete model see S2). The first number is the flux in the N402 strain and the second number (italic) is the flux in the N402 strain with 50 mM malonate added. G6P = glucose-6-phosphate, F6P = fructose-6-phosphate, GOL = glycerol, G3P = glyceraldehydes-3-phosphate, PEP = phosphoenolpyruvate, PYR_{cyt} = cytosolic pyruvate, SER = serine, GLY = glycine, THR = threonine, OAA_{cyt} = cytosolic oxaloacetate, CIT = citrate, $ACCoA_{cyt}$ = cytosolic acetyl-CoA, OXA_{cyt} = cytosolic oxalate, $ACCoA_{mit}$ = mitochondrial acetyl-CoA, OAA_{cyt} = mitochondrial oxaloacetate, AkGT = alfa-keto-glutarate, SUC = succinate, FUM = fumarate and MAL = malate.

parallel pathway to the TCA cycle and by up-regulation of the glyoxylate bypass the flux through the TCA cycle was expected to decrease. Even though flux analysis showed a decreased flux through the TCA cycle, more fumarate was produced instead of malate and succinate. This change in organic acid profiles was caused by regulation within the TCA cycle and not by the glyoxylate bypass.

A second method for stimulating the glyoxylate bypass was investigated. Malonate inhibits the SDH, which should lead to succinate production. The addition of malonate showed different cellular effects in both the WT and ICL over-expression strain. In the WT, the malonate addition resulted in more citrate and oxalate production, while in the ICL over-expression strain more malate was produced.

The combination of flux, gene expression, enzyme activity and metabolite production data gave a better understanding of the physiological behaviour of the cells and resulted in some unexpected outcomes. The hypothesised increase in glyoxylate bypass by over-expression of *icl* and its influence of succinate and malate showed distinct results. This shows that there is a

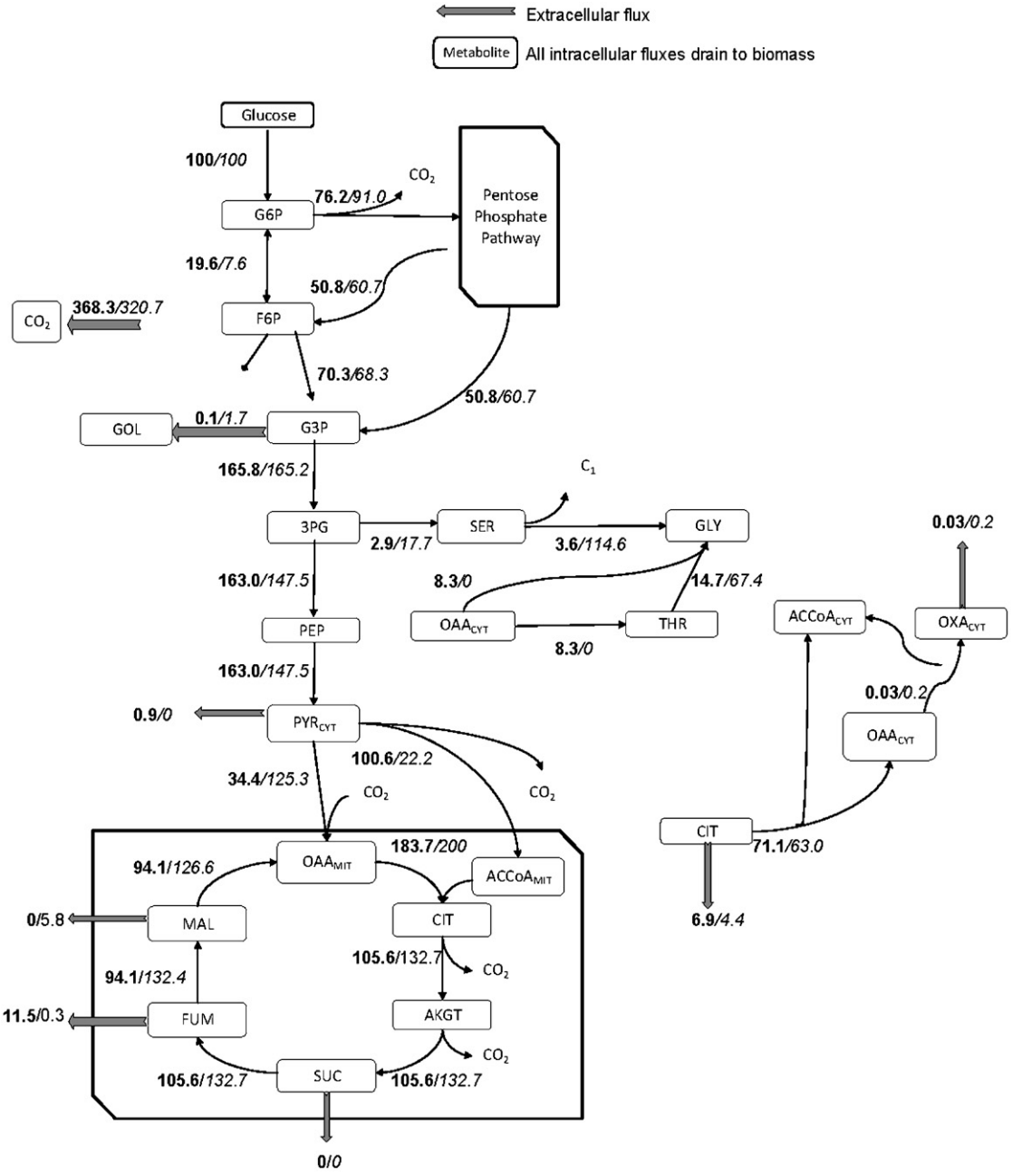

Fig. 4. A simplified flux distribution model of the ICL over-expression strain with and without 50 mM malonate addition (complete model see S2). The first number is the flux in the ICL over-expression strain and the second number (italic) is the flux in the ICL over-expression strain with 50 mM malonate added. G6P = glucose-6-phosphate, F6P = fructose-6-phosphate, GOL = glycerol, G3P = glyceraldehydes-3-phosphate, PEP = phosphoenolpyruvate, PYR_{cyt} = cytosolic pyruvate, SER = serine, GLY = glycine, THR = threonine, OAA_{cyt} = cytosolic oxaloacetate, CIT = citrate, $ACCoA_{cyt}$ = cytosolic acetyl-CoA, OXA_{cyt} = cytosolic oxalate, $ACCoA_{mit}$ = mitochondrial acetyl-CoA, OAA_{cyt} = mitochondrial oxaloacetate, AkGT = alfa-keto-glutarate, SUC = succinate, FUM = fumarate and MAL = malate.

coordinated regulation of fluxes through the glycolysis, the TCA cycle and different anapleorotic reactions, and redirection of the carbon fluxes therefore requires building better models for the overall regulation in these pathways. In order to stimulate succinate production in *A. niger* a better understanding of the transport mechanisms is required, since compartmentalization plays an important role in determining the flux distribution. Another important aspect is the enzyme reaction performed by the fumarate reductase. This enzyme is thought to be very inefficient in *A. niger* and stimulating this reaction will probably lead to an increased flux through the reductive branch of the TCA cycle and hereby lead to an increased succinic acid production.

Appendix A. Supplementary materials

Supplementary data associated with this article can be found in the online version at doi:10.1016/j.ymben.2008.12.002.

References

Affymetrix, 2007. GeneChip expression analysis technical manual—with specific protocols for using the GeneChip hybridisation, wash, and stain kit. P/N 702232 Rev 2.

Andersen, M.R., Vongsangnak, W., Panagiotou, G., Salazar, M.P., Lehmann, L., Nielsen, J., 2008. A tri-species *Aspergillus* microarray: comparative transcriptomics of three *Aspergillus* species. PNAS 105, 4387–4392.

Armson, A., Grubb, W.B., Mendis, A.H.W., 1995. The effect of electron-transport (Et) inhibitors and thiabendazole on the fumarate reductase (FR) and succinate dehydrogenase (SDH) of *Strongyloides ratti* infective (L3) larvae. Int. J. Parasitol. 25, 261–263.

Baker, S.E., 2006. *Aspergillus niger* genomics: past, present and into the future. Med. Mycol. 44, S17–S21.

Benjamini, Y., Hochberg, Y., 1995. Controlling the false discovery rate—a practical and powerful approach to multiple testing. Journal of the Royal Statistical Society Series B-Methodological 57, 289–300.

Bolstad, B.M., Irizarry, R.A., Astrand, M., Speed, T.P., 2003. A comparison of normalisation methods for high density oligonucleotide array data based on variance and bias. Bioinformatics 19, 185–193.

Bradford, M.M., 1976. Rapid and sensitive method for quantitation of microgram quantities of protein utilizing principle of protein–dye binding. Anal. Biochem. 72, 248–254.

Bowyer, P., De Lucas, J.R., Turner, G., 1994. Regulation of the expression of the isocitrate lyase gene (acuB) of *Aspergillus nidulans*. Mol. Gen. Genet. 242, 484–489.

Christensen, B., Nielsen, J., 1999. Isotopomer analysis using GC–MS. Metab. Eng. 1, 282–290.

Cleland, W.W., Johnson, M.J., 1954. Tracer experiments on the mechanism of citric acid formation by *Aspergillus niger*. J. Biol. Chem. 208, 679–689.

Führer, L., Kubicek, C.P., Rohr, M., 1980. Pyridine nucleotide levels and ratios in *Aspergillus niger*. Can. J. Microbiol. 26, 411.

Gautier, L., Cope, L., Bolstad, B.M., Irizarry, R.A., 2004. Affy-analysis of Affymetrix GeneChip data at the probe level. Bioinformatics 20, 307–315.

Grotkjaer, T., Christakopoulos, P., Nielsen, J., Olsson, L., 2005. Comparative metabolic network analysis of two xylose fermenting recombinant *Saccharomyces cerevisiae* strains. Metab. Eng. 7, 437–444.

Hatefi, Y., Stiggall, D.L., 1976. Metal-containing flavoprotein dehydrogenase. In: Boyer, P.D. (Ed.), The enzymes, vol. 13, pp. 175–297.

Irizarry, R.A., Hobbs, B., Collin, F., Beazer-Barclay, Y.D., Antonellis, K.J., Scherf, U., Speed, T.P., 2003. Exploration, normalisation, and summaries of high density oligonucleotide array probe level data. Biostatistics 4, 249–264.

Kornberg, H.L., Krebs, H.A., 1957. Synthesis of cell constituents from C2-units by a modified tricarboxylic acid cycle. Nature 179, 988–991.

Kornberg, H.L., 1966. Role and control of glyoxylate bypass in *Escherichia coli*—first Colworth Medal Lecture. Biochem. J. 99, 1–11.

Kristiansen, B., Mattey, M., Linden, J., 1999. Biochemistry of citric acid accumulation by *A. niger*. In: Kristiansen, B., Mattey, M., Linden, J. (Eds.), Citric Acid Biotechnology. Taylor & Francis, London.

Kubicek, C.P., Rohr, M., 1977. Influence of manganese on enzyme synthesis and citric acid accumulation in *Aspergillus niger*. Eur. J. Appl. Microbiol. 4, 167–175.

Kubicek, C.P., Rohr, M., 1980. Regulation of citrate synthase from the citric acid-accumulating fungus, *Aspergillus niger*. Biochim. Biophys. Acta 615, 449–457.

Legisa, M., Mattey, M., 1986. Glycerol synthesis by *Aspergillus niger* under citric acid accumulating conditions. Enzyme Microb. Technol. 8, 607–609.

Martin, S.M., Wilson, P.W., 1951. Uptake of C^{14}-O_2 by *Aspergillus niger* in the formation of citric acid. Arch. Biochem. Biophys. 32, 150–157.

Meijer, S., Panagiotou, G., Olsson, L., Nielsen, J., 2007. Physiological characterisation of xylose metabolism in *Aspergillus niger* under oxygen-limited conditions. Biotechnol. Bioeng. 98, 462–475.

Nielsen, M.L., Albertsen, L., Lettier, G., Nielsen, J.B., Mortensen, U.H., 2006. Efficient PCR-based gene targeting with a recyclable marker for *Aspergillus nidulans*. Fungal Genet. Biol. 43, 54–64.

Papagianni, M., 2007. Advances in citric acid fermentation by *Aspergillus niger*: biochemical aspects, membrane transport and modelling. Biotechnol. Adv. 25, 244–263.

Pel, H.J., de Winde, J.H., Archer, D.B., Dyer, P.S., Hofmann, G., Schaap, P.J., Turner, G., de Vries, R.P., Albang, R., Albermann, K., Andersen, M.R., Bendtsen, J.D., Benen, J.A.E., van den Berg, M., Breestraat, S., Caddick, M.X., Contreras, R., Cornell, M., Coutinho, P.M., Danchin, E.G.J., Debets, A.J.M., Dekker, P., van Dijck, P.W.M., van Dijk, A., Dijkhuizen, L., Driessen, A.J.M., d'Enfert, C., Geysens, S., Goosen, C., Groot, G.S.P., de Groot, P.W.J., Guillemette, T., Henrissat, B., Herweijer, M., van den Hombergh, J.P.T.W., van den Hondel, C.A.M.J., van der Heijden, R.T.J.M., van der Kaaij, R.M., Klis, F.M., Kools, H.J., Kubicek, C.P., van Kuyk, P.A., Lauber, J., Lu, X., van der Maarel, M.J.E.C., Meulenberg, R., Menke, H., Mortimer, M.A., Nielsen, J., Oliver, S.G., Olsthoorn, M., Pal, K., van Peij, N.N.M.E., Ram, A.F.J., Rinas, U., Roubos, J.A., Sagt, C.M.J., Schmoll, M., Sun, J.B., Ussery, D., Varga, J., Vervecken, W., de Vondervoort, P.J.J.V., Wedler, H., Wosten, H.A.B., Zeng, A.P., van Ooyen, A.J.J., Visser, J., Stam, H., 2007. Genome sequencing and analysis of the versatile cell factory *Aspergillus niger* CBS 513.88. Nat. Biotechnol. 25, 221–231.

R Development Core Team, 2007. R: A Language and Environment for Statistical Computing. R Foundation for Statistical Computing, Vienna, Austria 〈http://www.R-project.org〉.

Ruijter, G.J.G., Kubicek, C.P., Visser, J., 2002. Production of organic acids by fungi. In: Esser, K., Bennet, J.W. (Eds.), The Mycota, Industrial Applications. Springer, Berlin, pp. 213–230.

Schmidt, K., Carlsen, M., Nielsen, J., Villadsen, J., 1997. Modelling isotopomer distributions in biochemical networks using isotopomer mapping matrices. Biotechnol. Bioeng. 55, 831–840.

Smith, C.A., Want, E.J., O'Maille, G., Abagyan, R., Siuzdak, G., 2006. XCMS: processing mass spectrometry data for metabolite profiling using nonlinear peak alignment, matching, and identification. Anal. Chem. 78, 779–787.

Smyth, G.K., 2004. Linear models and empirical Bayes methods for assessing differential expression in microarray experiments. Stat. Appl. Genet. Mol. Biol. 3 (Article 3).

Vanhartingsveldt, W., Mattern, I.E., vanZeijl, C.M.J., Pouwels, P.H., vanden Hondel, C.A.M.J., 1987. Development of a homologous transformation system for *Aspergillus niger* based on the pyrG gene. Mol. Gen. Genet. 206, 71–75.

Werpy, T., Petersen, G., 2004. Top value added chemicals from biomass. 〈http://www.nrel.gov/docs/fy04osti/35523.pdf〉 (27-03-2008).

Wiechert, W., 2001. C^{13} metabolic flux analysis. Metab. Eng. 3, 195–206.

Zupke, G., Stephanopoulos, G.N., 1994. Modelling of isotope distributions and intracellular fluxes in metabolic networks using atom mapping matrices. Biotechnol. Prog. 10, 89–498.